PHYSICAL REVIEW B VOLUME 6, NUMBER 7 1 OCTOBER 1972

Magnetic Excitons in Real Singlet-Ground-State Ferromagnets: Application to Pr_3Tl and fcc Pr

Bernard R. Cooper
General Electric Research and Development Center, Schenectady, New York 12301
(Received 21 March 1972)

We have studied the magnetic-exciton behavior expected in cubic systems containing Pr^{3+} with a crystal-field-only Γ_1 singlet ground state. We use this study to discuss the experimentally observed behavior in Pr_3Tl and fcc Pr. In particular, we show that crystal-field states lying higher than the Γ_4 first-excited triplet have an important qualitative effect on the magnetic-exciton dispersion relationship. The most important difference from the results for a singlet-triplet model is the appearance of a substantial gap at $\vec{q}=0$ (~ 18 °K in a typical realistic case) for the transverse excitons in the ferromagnetic state; while the gap for the longitudinal modes would also be much different if one neglected the higher-lying crystal-field states ($\sim 75\%$ greater in a typical realistic case). The necessity of including effects of crystal-field states above the Γ_4 triplet led us to adopt an effective boson (i.e., Bogoliubov-type) approximation valid only as the temperature approaches zero. We then use our knowledge of the random-phase-approximation (RPA) results for the singlet-singlet problem to discuss the expected temperature dependence of the excitation spectrum. The existing theory, including the effects of all crystal-field levels, is quite successful in quantitatively predicting the experimental magnetic-exciton behavior at low temperature in Pr_3Tl. On the other hand, the existing theory offers no explanation for the absence of any measurable change with temperature of the measured dispersion relationship even when going to temperature well above the Curie temperature in Pr_3Tl and fcc Pr. Incidental to our discussion of the magnetic-exciton behavior, we treat the macroscopic magnetization variation with temperature in Pr_3Tl including all crystal-field levels in a molecular-field theory.

I. INTRODUCTION

For several years there has been much interest in the magnetic behavior of systems with crystal-field-only singlet ground states.[1] There have been theoretical studies of both the macroscopic magnetic properties of such systems[2-5] and of the collective-excitation (magnetic-exciton) behavior.[2,5,6-10] For the most part these calculations have been for model singlet-singlet systems (i.e., where the only excited state considered is also a crystal-field-only singlet), or, to a lesser extent, for model singlet-triplet systems. There have been some molecular-field calculations for the macroscopic magnetization behavior including the full crystal-field level scheme for real systems,[11] but there has been essentially no work including the effects of the full crystal-field level scheme on the dispersion relationships for the collective excitations, i.e., the magnetic excitons. Until quite recently the experimental studies of such materials have been entirely on the macroscopic magnetic properties. However, within the past year experimental studies of the collective excitations by neutron inelastic scattering have begun to appear.[12-15] In particular, the striking magnetic-exciton behavior of fcc Pr and Pr_3Tl has been reported.[14,15] An attempt to understand the results of these experiments calls for inclusion of the effects of the full crystal-field level scheme. The exciton behavior expected including such effects is qualitatively different in one important respect from the results for a singlet-triplet model. This is the appearance of a gap at $\vec{q}=0$ for the transverse excitons in the ferromagnetic state. The existing theory, including the effects of all crystal-field levels as described below, is quite successful in quantitatively describing the experimental magnetic-exciton behavior at low temperatures in Pr_3Tl. Indeed, the results of calculations given in Sec. III, although not previously reported, were done some months before the experiments, and successfully predicted their results. The agreement with the behavior of fcc Pr at low temperature is not quite as good; however, this is probably related to the experimental ambiguity[14,15] with regard to the details of magnetic ordering in fcc Pr. On the other hand, the existing theory offers no explanation for the absence of any measurable change with temperature of the measured dispersion relationship even when going to temperature well above the Curie temperature in Pr_3Tl and fcc Pr. (This lack of any mode softening is in contrast with the reported behavior[13] in paramagnetic dhcp Pr, where there is evidence for mode softening on going to low temperature.)

The contents of the present paper are as follows. In Sec. II we first briefly review the experimental situation for the macroscopic magnetic properties of Pr_3Tl and fcc Pr. We describe our basic model

and assumptions for treating the equilibrium and dynamic magnetic behavior of these materials, and then relate the expected behavior of the macroscopic magnetization, including crystal-field effects, to the experimental behavior. In Sec. III we discuss the low-temperature exciton behavior expected for crystal-field parameters near the value of x, the parameter specifying the ratio of fourth- to sixth-order anisotropy, pertaining on a point-charge picture, $x=-0.877$. For this value of x the first-excited crystal-field state is a Γ_4 triplet, and the Γ_5 triplet lies well above the Γ_4 state. We show that, using the experimental crystal-field splitting and ordered moment at $T=0$ as the only adjustable parameters, we predict magnetic-exciton behavior for Pr_3Tl in close agreement with experiment. In Sec. IV we discuss the situation for values of x near the Γ_4-Γ_5 crossing, which occurs at $x=-0.375$. Here, the transverse excitons involve strong mixing of the Γ_4 and Γ_5 states. (The longitudinal-exciton behavior is independent of x.) The exciton behavior found for x near the Γ_4-Γ_5 crossing does not describe the experimental behavior. This, coupled with the agreement of theory and experiment for x near the point-charge value as discussed in Sec. III, indicates the dominance of fourth-order crystal-field effects as predicted by the point-charge model and found experimentally in a number of rare-earth intermetallic compounds.[16-21] In Sec. V we discuss the expected temperature variation of the theoretical exciton spectra found in Secs. III and IV, and the failure of the theoretical behavior to describe the experimental lack of temperature dependence.

II. CRYSTAL-FIELD LEVEL STRUCTURE AND MACROSCOPIC MAGNETIC PROPERTIES OF fcc Pr and Pr_3Tl

A. Basic Model and Assumptions

For Pr_3Tl the neutron investigations of Birgeneau *et al.*[14,15] find a Curie temperature of (11.6 ± 0.3) °K in good agreement with the value of 11.3 °K found in the susceptibility measurements of Andres *et al.*[22] The ordering appears to be simple ferromagnetism, and the transition is second order.[14,15,22,23] The susceptibility measurements indicate an ordered moment at very low temperature of about 0.22 of the free-ion moment of Pr^{3+} ($3.2\mu_B$); while the neutron measurements indicate a larger value, about 0.30 of the free-ion moment. For fcc Pr the bulk magnetization measurements of Bucher *et al.*[24] indicate a ferromagnetic transition at 8.7 °K; however, the situation is more complicated. There is remanence persisting up to 20 °K, and neutron measurements[14,15] indicate a second magnetic phase transition at (20 ± 2)°K. The ordered moment per Pr ion as T approaches 0 °K is somewhere between 0.20 and 0.25 of the free-ion moment of Pr^{3+}.

The crystal-field Hamiltonian for a rare-earth ion in a cubic crystal-field has the form[25]

$$\mathcal{H}_{CF}=B_4(O_4^0+5\times O_4^4)+B_6(O_6^0-21\times O_6^4)\ . \qquad (2.1)$$

Here O_4^0, O_4^4, O_6^0, and O_6^4 are specified operators for a given J ($J=4$ for Pr^{3+}), and the axis of quantization has been chosen parallel to a cubic crystal axis. The operators O_4^0 and O_4^4 are fourth-order in the components of $\vec{J}$, while O_6^0 and O_6^4 are sixth-order in $\vec{J}$. Thus, the crystal-field Hamiltonian is completely determined by symmetry considerations except for the parameters B_4 and B_6. Rather than deal with B_4 and B_6, it is more convenient to treat two other parameters,[25] x and W. The ratio of fourth- to sixth-order anisotropy is given by x; while W gives the absolute scaling of the crystal-field energy levels:

$$B_4/B_6\equiv[x/(1-|x|)][F(6)/F(4)]\ , \qquad (2.2)$$

$$B_4F(4)\equiv Wx\ . \qquad (2.3)$$

Here $F(4)$ and $F(6)$ are numerical factors known for a given J.

In Fig. 1 we reproduce[25] the variation of crystal-field energy (in units of W) with x for Pr^{3+}. Pr_3Tl has the Cu_3Au crystal structure. Each Pr site has four Tl nearest neighbors and eight Pr nearest neighbors arranged as on an fcc lattice. So if we ignore the difference in effective charge on Pr and Tl, the crystal field acting on a Pr^{3+} ion in Pr_3Tl behaves in the same way as in an fcc lattice. Thus, in the nearest-neighbor point-charge model the crystal-field parameters for both fcc Pr and Pr_3Tl are given by the same expressions[26]:

$$B_4=\tfrac{7}{32}(|e|q/d^5)\beta_J\langle r^4\rangle\ , \qquad (2.4a)$$

$$B_6=\tfrac{39}{256}(|e|q/d^7)\beta_J\langle r^6\rangle\ . \qquad (2.4b)$$

Here $|e|$ is the electron charge, q is the nearest-neighbor charge, d is the distance to a nearest-

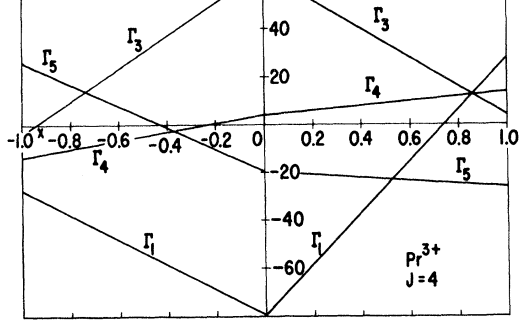

FIG. 1. E/W vs x for $J=4$, applicable to Pr^{3+} (after Ref. 25).

neighbor, β_J and γ_J are specified constants for specified J($J=4$ for Pr^{3+}), and $\langle r^4\rangle$ and $\langle r^6\rangle$ are the average values[27] of r^4 and r^6 for an f electron on the Pr^{3+} ion.[28]

We use the point-charge expressions only in considering the ratio of fourth-order to sixth-order terms. The magnitude of the crystal-field splitting is set by the experimental behavior. Then,

$$B_4/B_6 = \tfrac{7}{32}\,\tfrac{256}{39}\,d^2(\beta_J/\gamma_J)(\langle r^4\rangle/\langle r^6\rangle)\ . \qquad (2.5)$$

Note that this expression is independent of the sign and size of the effective nearest-neighbor point charge. Using the lattice parameter[24] (5.186 Å) of fcc Pr, the known values of β_J and γ_J, and Freeman and Watson's[27] calculated values for $\langle r^4\rangle$ and $\langle r^6\rangle$ gives

$$x = -0.877, \quad \text{point-charge model.} \qquad (2.6)$$

(The lattice constant of Pr_3Tl is about 5% less than that of fcc Pr. This gives a value of x about 1% smaller in magnitude, a negligible difference so far as affecting any of the magnetic properties is concerned.)

We used this value of x in our first considerations of the magnetic-exciton behavior. Subsequently, we also considered values of x near the Γ_4-Γ_5 crossover. As discussed in Secs. III and IV, the point-charge value of x leads to a low-temperature exciton spectrum in Pr_3Tl, very close to the experimental behavior at low T; while the dispersion curves for x closer to zero (i.e., near the Γ_4-Γ_5 crossover) do not agree with experiment. For this reason, we discuss the bulk magnetization behavior of Pr_3Tl for x given by the point-charge value. Actually, the bulk magnetic properties are not particularly sensitive to the value of x.

The model used in our calculations does not predict different behavior for Pr_3Tl and fcc Pr, since the only parameters used are the crystal-field splitting and the ordered moment per Pr^{3+} at $T=0$, and both these quantities are about the same for Pr_3Tl and fcc Pr. However, these seem to be rather significant differences between the experimental behavior of Pr_3Tl and fcc Pr. This may be because the ordering of fcc Pr is not simple ferromagnetism. For this reason all of our detailed comparisons with experiment for both the macroscopic magnetization and the magnetic excitons are for Pr_3Tl rather than for fcc Pr.

Analyzing the specific-heat measurements on fcc Pr in terms of sharp energy levels for the Pr^{3+} ion indicates that the splitting to the first crystal-field level (Δ) is[24] 69 ± 4 °K; while considering that one has a dispersion curve, as measured in the neutron experiments, rather than a sharp crystal-field excited state could give a Δ as high as[14,15] 80 °K. For $(Pr_xLa_{1-x})_3Tl$, susceptibility measurements on samples dilute in Pr indicate a Δ of about[23] 65 °K, while consideration of the exciton dispersion again might give a Δ more like[14,15] 80 °K. Specific-heat measurements[23] also lead to an estimate $\Delta\sim 80$ °K for Pr_3Tl. Our calculations were initiated and largely completed when the only experimental information available on Δ was from the specific-heat work on fcc Pr. For that reason we have used $\Delta = 69$ °K in all our calculations. (*For all values of x we have considered, the first excited state is always* Γ_4; *so* Δ *is always the* Γ_4-Γ_1 *splitting in Fig.* 1.) This falls within the narrow range indicated by the various experiments. (The results we find for the exciton behavior at $T=0$ °K in Sec. III indicate the value of Δ might be a few °K larger, but this is a difference of no real significance.)

For our treatment of the equilibrium and dynamic magnetic behavior of Pr_3Tl and fcc Pr we assume a Hamiltonian consisting of a crystal-field term and an isotropic exchange term. (The exchange may very well be anisotropic, but this assumption gives us something concrete to work with.) Anisotropic exchange effects would make no qualitative difference unless rather large. The *a posteriori* agreement of the magnetization vs T and low-T magnetic-exciton behavior for Pr_3Tl indicates that our assumption that anisotropic exchange effects are not large enough to change the behavior qualitatively is justified. The fact that biquadratic exchange does not couple Γ_1 to Γ_4 except by higher-order processes would tend to minimize the effects of any such interaction. (Biquadratic exchange means that the effective spin operator on site i is quadratic and, therefore, $\sim\Gamma_3+\Gamma_5$. Note, however, that the fact, discussed below, that the molecular-field Γ_3 admixture to the ground state has significant effects on the soft-mode behavior indicates that higher-order exchange processes cannot in general be ignored for these systems.) Also, the fact that the neutron scattering experiments are on powder samples would tend to average out any anisotropic exchange effects:

$$\mathcal{H} = \sum_i V_{ci} - \sum_{i\neq j} \mathcal{J}_{ij}\vec{J}_i\cdot\vec{J}_j\ . \qquad (2.7)$$

Here the first term is the crystal-field Hamiltonian of (2.1) summed over all Pr^{3+} sites, and the second term is an isotropic exchange interaction.

We separate this Hamiltonian into a molecular-field Hamiltonian $\mathcal{H}_0$ and a contribution $\mathcal{H}_1$, giving the correction between the molecular-field Hamiltonian and the exact Hamiltonian:

$$\mathcal{H} = \mathcal{H}_0 + \mathcal{H}_1\ , \qquad (2.8a)$$

$$\mathcal{H}_0 = \sum_i [V_{ci} - 2\mathcal{J}(0)\langle J\rangle J_{zi}] + N\mathcal{J}(0)\langle J\rangle^2\ , \qquad (2.8b)$$

$$\mathcal{H}_1 = -\sum_{i\neq j}\mathcal{J}_{ij}\vec{J}_i\cdot\vec{J}_j\ . \qquad (2.8c)$$

Here $\mathcal{J}(0)$ is the $\vec{q}=0$ component of the Fourier transform of the exchange energy,

$$\mathcal{J}(\vec{q})=\sum_j \mathcal{J}_{ij} e^{i\vec{q}\cdot\vec{r}_{ij}}, \tag{2.9}$$

and $\langle J\rangle$ is the thermal expectation value of J_z, where the z direction is chosen parallel to the direction of magnetization. Also, we have

$$\vec{j}_i=\vec{J}_i-\langle J\rangle\hat{\epsilon}_z \ , \tag{2.10}$$

where $\hat{\epsilon}_z$ is a unit vector along z.

We consider the equilibrium magnetization behavior on the basis of the molecular-field Hamiltonian $\mathcal{H}_0$. In Secs. III and IV, we will include the effect of $\mathcal{H}_1$ in considering the collective excitations.

Our basic physical picture is as follows. In zero applied field, we assume each crystallite has its magnetization along an easy axis. The easy axis for Pr_3Tl or fcc Pr for the range of x we consider is $\langle 100\rangle$, so the z direction, i.e., the axis of quantization and the direction of the exchange field, is $\langle 100\rangle$. (Presumably the $\langle 100\rangle$ axes of the various crystallites are randomly oriented with respect to one another, but that does not enter into our calculations.)

To determine the molecular-field states, we considered the mixing of the crystal-field-only states, where the splitting to the first excited (Γ_4) state was set at 69 °K as given by Bucher *et al.*[24] The crystal-field-only wave functions[25] are:

$$\begin{aligned}
|\Gamma_1\rangle &= 0.4564|4\rangle+0.7638|0\rangle+0.4564|-4\rangle \ , \\
|\Gamma_{4b}\rangle &= 0.7071|4\rangle-0.7071|-4\rangle \ , \\
|\Gamma_{3a}\rangle &= 0.5401|4\rangle-0.6455|0\rangle+0.5401|-4\rangle \ ;
\end{aligned} \tag{2.11a}$$

$$\begin{aligned}
|\Gamma_{4a}\rangle &= 0.3536|3\rangle+0.9354|-1\rangle \ , \\
|\Gamma_{5a}\rangle &= 0.9354|3\rangle-0.3536|-1\rangle \ ;
\end{aligned} \tag{2.11b}$$

$$\begin{aligned}
|\Gamma_{4c}\rangle &= 0.3536|-3\rangle+0.9354|1\rangle \ , \\
|\Gamma_{5c}\rangle &= 0.9354|-3\rangle-0.3536|1\rangle ;
\end{aligned} \tag{2.11c}$$

$$\begin{aligned}
|\Gamma_{3b}\rangle &= 0.7071|2\rangle+0.7071|-2\rangle \ , \\
|\Gamma_{5b}\rangle &= 0.7071|2\rangle-0.7071|-2\rangle .
\end{aligned} \tag{2.11d}$$

Here the states on the right are identified by their J_z quantum numbers, and we have arranged the states into four groups. The molecular field along the z axis admixes the states within each of these groups. The crystal-field-only energy eigenvalues (for $-1\leq x\leq 0$) are:

$$\begin{aligned}
E(\Gamma_1)&=(-80-52x)W, \qquad E(\Gamma_4)=(4+18x)W, \\
E(\Gamma_3)&=(64+68x)W, \qquad E(\Gamma_5)=(-20-46x)W.
\end{aligned} \tag{2.12}$$

Note that the Γ_3-Γ_4 splitting is always $\frac{5}{7}$ of the Γ_4-Γ_1 splitting, so that if $E(\Gamma_4)-E(\Gamma_1)$ is kept constant on varying x, $E(\Gamma_3)-E(\Gamma_4)$ is also kept constant.

To determine the molecular-field states, we first specified $x=0.877$ (the point-charge value). Setting $E(\Gamma_4)-E(\Gamma_1)=69$ °K then gave $W=3.052$ °K completely specifying the crystal-field level scheme.

To determine the exchange field,

$$g\mu_B H_{ex}=2\mathcal{J}(0)\langle J\rangle, \tag{2.13a}$$

necessary to find the molecular-field states [and also giving $\mathcal{J}(0)$], we used the experimental value of the ordered moment at $T\approx 0$. The value for this moment found in neutron experiments[14,15] is somewhat less than that found by bulk susceptibility measurements[22,23] in fcc Pr and somewhat greater in Pr_3Tl. We used a value of $M(T=0)\equiv M_0=0.75\mu_B$, closer to the bulk susceptibility value[22,24] in both fcc Pr and Pr_3Tl. We then calculated the molecular field states and the expectation value of J_z in the molecular-field ground state $|1_m\rangle$, for varying values of H_{ex}. We found that $H_{ex}=9.155\times 10^4$ Oe gave $g\mu_B\langle 1_m|J_z|1_m\rangle=0.75\,\mu_B$ Once H_{ex} is specified, $\mathcal{J}(0)$ is determined from (2.13) with $\langle J\rangle=\langle 1_m|J_z|1_m\rangle$. This gives

$$\mathcal{J}(0)=2.623\ ^\circ\mathrm{K} \ . \tag{2.13b}$$

To give the reader some feeling for the degree of mixing of the crystal-field states involved in arriving at the molecular-field states, and for later reference, we give the molecular-field states for $x=-0.877$, $W=3.052$ °K, and $H_{ex}=9.155\times 10^4$ Oe (giving $M_0=0.75\mu_B/\mathrm{Pr}$):

$$\begin{aligned}
&E_1=-107.3\ ^\circ\mathrm{K}, \\
&|1_m\rangle=0.9834|\Gamma_1\rangle+0.1799|\Gamma_{4b}\rangle+0.0224|\Gamma_{3a}\rangle; \\
&E_2=-38.0\ ^\circ\mathrm{K}, \\
&|2_m\rangle=-0.1790|\Gamma_1\rangle+0.9441|\Gamma_{4b}\rangle+0.2767|\Gamma_{3a}\rangle \ ; \\
&E_3=17.6\ ^\circ\mathrm{K}, \\
&|3_m\rangle=0.0286|\Gamma_1\rangle-0.2762|\Gamma_{4b}\rangle+0.9607|\Gamma_{3a}\rangle \ ; \\
&E_4=-34.0\ ^\circ\mathrm{K} \ , \\
&|4_m\rangle=0.9970|\Gamma_{4a}\rangle+0.0774|\Gamma_{5a}\rangle \ ; \\
&E_5=50.3\ ^\circ\mathrm{K} \ , \\
&|5_m\rangle=-0.0774|\Gamma_{4a}\rangle+0.9970|\Gamma_{5a}\rangle; \\
&E_6=-38.8\ ^\circ\mathrm{K}, \\
&|6_m\rangle=0.9984|\Gamma_{4c}\rangle-0.0574|\Gamma_{5c}\rangle; \\
&E_7=74.8\ ^\circ\mathrm{K} \ , \\
&|7_m\rangle=0.0574|_{4c}\rangle+0.9984|\Gamma_{5c}\rangle; \\
&E_8=11.4\ ^\circ\mathrm{K} \ , \\
&|8_m\rangle=0.9817|\Gamma_{3b}\rangle+0.1906|\Gamma_{5b}\rangle; \\
&E_9=64.0\ ^\circ\mathrm{K}, \\
&|9_m\rangle=-0.1906|\Gamma_{3b}\rangle+0.9817|\Gamma_{5b}\rangle .
\end{aligned} \tag{2.14}$$

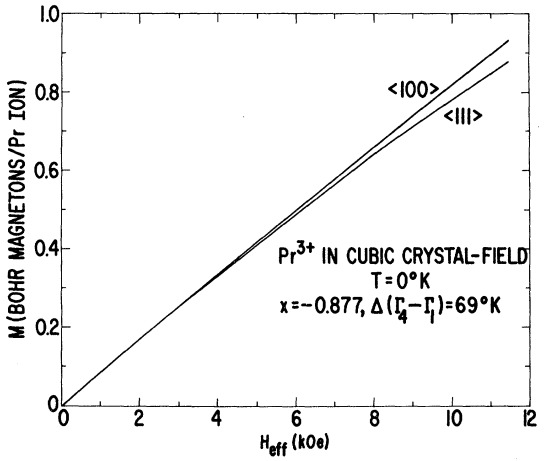

FIG. 2. Magnetization of Pr^{3+} for $x=-0.877$, $\Delta(\Gamma_4-\Gamma_1)=69\,^\circ\mathrm{K}$ at $T=0$.

This gives the molecular-field states for the value of H_{ex} giving the behavior at $T=0$. Figure 2 shows the variation of M with H_{ex} at $T=0$. At any specified temperature the magnetic moment per Pr^{3+} ion in Bohr magnetons is given by

$$M(H_{ex}, T)=(g\sum_{n=1}^{9}\langle n_m|J_z|n_m\rangle e^{-E_n/T})/\sum_{n=1}^{9}e^{-E_n/T}\,, \tag{2.15}$$

where E_n is in units of °K. Thus, one produces a curve of the form shown in Fig. 2 for any given temperature. While only the ⟨100⟩ easy magnetization curve is relevant to the present discussion, we also show the ⟨111⟩ hard direction curve. We note that at the exchange fields relevant to the behavior of Pr_3Tl or fcc Pr there is little anisotropy; an additional 5 kOe brings the magnetization in the hard direction up to that in the easy direction. (We have also verified that ⟨100⟩ is the easy direction, and the small size of anisotropy, for the value $x=-0.425$ near the Γ_5-Γ_4 crossing.) This accounts for the behavior noted by Andres *et al.*[22] that magnetic "saturation" is achieved in comparatively low fields, indicating a small magnetic anisotropy. As we have noted elsewhere,[5] the anisotropy in the magnetization arises from the presence of excited crystal-field states in addition to the Γ_4 triplet.

Simultaneously satisfying (2.13a) and (2.15) at any T determines M, and also H_{ex}, at that T. This gives the curve of M/M_0 vs T shown in Fig. 3, which is in reasonable semiquantitative agreement with the experimental behavior for Pr_3Tl found by the neutron measurements.[15] (The value we assumed for M_0, $0.75\mu_B$, is close to that found in susceptibility experiments[22] with the Pr diluted by La; and is lower than the value of close to $1\mu_B$ found in the neutron experiments.[15]) The difference between the theoretical and experimental curves corresponds to the fact that the theoretical value of the Curie temperature is 14.4 °K compared to the experimental value[15] of 11.6 °K. This difference probably reflects the limitations of a molecular-field treatment, particularly when the Curie temperature is in a regime of behavior where it is sensitive to the values of exchange and crystal-field parameters.[1] (The magnetization-vs-temperature curve for fcc Pr deduced from neutron-scattering intensity measurements[29] has a much different shape than that for Pr_3Tl. This is presumably associated with peculiarities of magnetic behavior between 8 and 20 °K in fcc Pr, and we do not discuss this here.)

The theoretical value of T_C has a fairly significant difference from the value obtained by including only the Γ_4 excited state. For the singlet-triplet model, T_C is given by

$$T_C'=\Delta\ln\left(\frac{[1-(\Delta/4\alpha^2T_C')]+3[1-(M_0/g\alpha)^2]^{1/2}}{1-[1-(M_0/g\alpha)^2]^{1/2}}\right)^{-1}. \tag{2.16}$$

Here $\alpha\equiv\langle\Gamma_1|J_z|\Gamma_{4b}\rangle=2.5818$, and M_0 is the ordered moment at $T=0$. [The $(\Delta/4\alpha^2T_C')$ term was omitted by Bucher *et al.*[24] and changes the value of T_C only by about 1%.] From (2.16) one obtains $T_C=17.4\,^\circ\mathrm{K}$ for the singlet-triplet model for the same Δ and M_0 as used to obtain 14.4 °K using the full crystal-field level scheme.

III. EXCITATION SPECTRUM FOR $x=-0.887$ (POINT-CHARGE VALUE)

In investigating the theoretically expected excitation spectrum for fcc Pr and Pr_3Tl, we anticipated that it would be necessary to include the effects of the full crystal-field level scheme. Furthermore, we anticipated that for values of x not too far from $x=-1$ (fourth-order anisotropy only), while the effects of the crystal-field states lying higher than the Γ_4-triplet would be important in finding the correct molecular-field states, once the molecular-field states are found, to a good approximation only the molecular-field states derived primarily from the Γ_4 state [states $|2_m\rangle$, $|4_m\rangle$, and $|6_m\rangle$ of Eq. (2.14)] would give rise to strongly magnetic-dipole-excited collective excitations showing substantial dispersion. The higher-lying molecular-field states were expected to give rise to weak but sharp excitations. On the other hand, for x near the value for the Γ_4-Γ_5 crossing (see Fig. 1), for the transverse modes we expected strong mixing of the molecular-field states with parentage from the Γ_4 and Γ_5 states (states $|4_m\rangle$, $|5_m\rangle$, $|6_m\rangle$, and $|7_m\rangle$), and that finding the transverse collective excitation behavior would involve including molecular-field states including all mixing effects of the Γ_4 and Γ_5 states. We will now show that all of our expectations outlined above were justified.

The necessity of including effects of crystal-

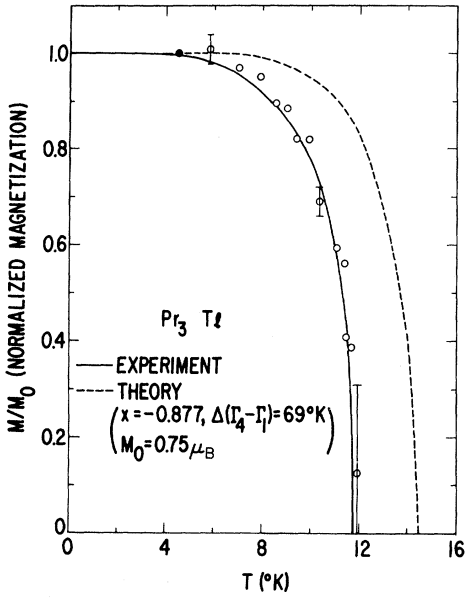

FIG. 3. Normalized magnetization vs temperature for Pr_3Tl. Experimental data are those of Fig. 3 of Ref. 15.

field states above the Γ_4 triplet led us to adopt an effective boson (i.e., Bogoliubov-type) approximation[2,6-8] to study the behavior at $T=0$. Such an approximation is valid only as T approaches zero. Alternatively, we could have attempted to develop some treatment like the random-phase-approximation (RPA) treatment for the singlet-triplet; however, abandoning self-consistency for the effective molecular field which always enters such a theory. We considered this a rather doubtful procedure; and, in any case, one could not treat strong mixing of the Γ_4 and Γ_5 states in such a calculation.

We begin by considering the longitudinal excitations for $x=-0.877$, the point-charge value. We retain all mixing effects between the molecular-field states $|1_m\rangle$, $|2_m\rangle$, and $|3_m\rangle$ of Eq. (2.14), and use this treatment to show that our anticipation was justified that only the mixing of $|1_m\rangle$ and $|2_m\rangle$ need be considered to find the strongly magnetic-dipole-excited states with substantial dispersion. We then consider the transverse excitons, including the mixing of $|1_m\rangle$, $|4_m\rangle$, and $|6_m\rangle$, which gives rise to the strongly magnetic-dipole-excited states with substantial dispersion. We show that the theoretical exciton dispersion curves for $x=-0.877$ are in excellent agreement with the low-temperature experimental results for Pr_3Tl. In Sec. IV we go on to consider the transverse exciton behavior for $x=-0.425$ near the Γ_4-Γ_5 crossing, where all mixing effects of the molecular-field states $|1_m\rangle$ with $|4_m\rangle$, $|5_m\rangle$, $|6_m\rangle$, and $|7_m\rangle$ must be included. This would predict quite different behavior than that for $x=-0.877$. Finally, in Sec. V we use our knowledge of the RPA results for the singlet-singlet problem to discuss the expected temperature dependence of the excitation spectrum. The experimental lack of temperature dependence is quite anomalous in the light of this discussion.

A. Longitudinal Excitations

The Bogoliubov-type approximation is based on separating the Hamiltonian, in the manner shown in Eq. (2.8), into a molecular-field Hamiltonian $\mathcal{H}_0$, and the difference $\mathcal{H}_1$ between that and the exact Hamiltonian.

We first express $\mathcal{H}_0$ in terms of fermion operators

$$\mathcal{H}_0=\sum_i\sum_{n=1}^{9}E_n d_{in}^\dagger d_{in}+N\mathcal{J}(0)\langle J\rangle^2 \quad , \tag{3.1}$$

where E_n are the molecular-field energies given by (2.14);

$$\mathcal{H}_0=\sum_i[E_1(1-\sum_{n=2}^{9}d_{in}^\dagger d_{in})+\sum_{n=2}^{9}E_n d_{in}^\dagger d_{in}]+N\mathcal{J}(0)\langle J\rangle^2$$

$$=N[E_1+\mathcal{J}(0)\langle J\rangle^2]+\sum_i\sum_{n=2}^{9}\epsilon_n d_{in}^\dagger d_{in} \quad , \tag{3.2}$$

where

$$\epsilon_n\equiv E_n-E_1, \quad n=2\text{–}9 \tag{3.3}$$

and defining the effective boson operators

$$a_{in}\equiv d_{i1}^\dagger d_{in}, \quad a_{in}^\dagger\equiv d_{in}^\dagger d_{i1} \tag{3.4}$$

gives

$$\mathcal{H}_0=N[E_1+\mathcal{J}(0)\langle J\rangle^2]+\sum_i\sum_{n=2}^{9}\epsilon_n a_{in}^\dagger a_{in} \quad . \tag{3.5}$$

Similarly, we can rewrite $\mathcal{H}_1$ in terms of the boson operators:

$$\mathcal{H}_1=\mathcal{H}_{1zz}+\mathcal{H}_{1+-} \quad , \tag{3.6}$$

where

$$\mathcal{H}_{1zz}=-\sum_{i\neq j}\mathcal{J}_{ij}j_{iz}j_{jz} \quad , \tag{3.7a}$$

$$\mathcal{H}_{1+-}=-\sum_{i\neq j}\mathcal{J}_{ij}J_{i+}J_{j-} \quad , \tag{3.7b}$$

$$\mathcal{H}_{1zz}=-\sum_{i\neq j}\mathcal{J}_{ij}\sum_n\sum_m(\langle 1|J_z|n\rangle d_{i1}^\dagger d_{in}+\langle n|J_z|1\rangle d_{in}^\dagger d_{i1})(\langle 1|J_z|m\rangle d_{j1}^\dagger d_{jm}+\langle m|J_z|1\rangle d_{jm}^\dagger d_{j1})$$

$$= -\sum_{i\neq j} \mathcal{J}_{in} \sum_n \sum_m (\langle 1|J_z|n\rangle a_{in} + \langle n|J_z|1\rangle a_{in}^\dagger)(\langle 1|J_z|m\rangle a_{jm} + \langle m|J_z|1\rangle a_{jm}^\dagger) \quad . \tag{3.8}$$

Since only $|2_m\rangle$ and $|3_m\rangle$ have nonzero matrix elements of J_z with $|1_m\rangle$,

$$\mathcal{H}_{1zz} = -\sum_{i\neq j} \mathcal{J}_{ij}[\langle 1|J_z|2\rangle(a_{i2}+a_{i2}^\dagger) + \langle 1|J_z|3\rangle(a_{i3}+a_{i3}^\dagger)][\langle 1|J_z|2\rangle(a_{j2}+a_{j2}^\dagger) + \langle 1|J_z|3\rangle(a_{j3}+a_{j3}^\dagger)] \, . \tag{3.9}$$

Thus, the boson Hamiltonian determining the longitudinal excitation energies consists of $\mathcal{H}_{1zz}$ plus the terms in $\mathcal{H}_0$ involving states $|1_m\rangle$, $|2_m\rangle$, and $|3_m\rangle$:

$$\mathcal{H}_{zz} = \sum_i (\epsilon_2 a_{i2}^\dagger a_{i2} + \epsilon_3 a_{i3}^\dagger a_{i3}) - \sum_{i\neq j} \mathcal{J}_{ij}[\langle 1|J_z|2\rangle^2 (a_{i2}^\dagger a_{j2}^\dagger + a_{i2}a_{j2} + 2a_{i2}^\dagger a_{j2})$$

$$+ \langle 1|J_z|3\rangle^2 (a_{i3}^\dagger a_{j3}^\dagger + a_{i3}a_{j3} + 2a_{i3}^\dagger a_{j3}) + 2\langle 1|J_z|2\rangle\langle 1|J_z|3\rangle (a_{i2}a_{j3} + a_{i2}^\dagger a_{j3}^\dagger + a_{i2}^\dagger a_{j3} + a_{i2}a_{j3}^\dagger)] \, . \tag{3.10}$$

In connection with Eq. (2.12) *we have already noted that the* Γ_3-Γ_4 *splitting is always* $\frac{5}{7}$ *of the* Γ_1-Γ_4 *splitting. Since in our calculations we keep* $E(\Gamma_4)$-$E(\Gamma_1)$ *constant on varying* x, *this means that the longitudinal exciton behavior is independent of* x.

With some moderately complicated algebra, one can actually diagonalize the Hamiltonian of (3.10) exactly in closed form after, of course, Fourier transforming.

We define the Fourier-transformed operators,

$$a_{qn} = N^{-1/2} \sum_i a_{in} e^{i\vec{q}\cdot\vec{r}_i} \tag{3.11}$$

and also define

$$A_{nq} \equiv \epsilon_n - 2\mathcal{J}(q)\langle 1_m|J_z|n_m\rangle^2, \quad n = 2, 3 \tag{3.12a}$$

$$B_{nq} \equiv \mathcal{J}(q)\langle 1_m|J_z|n_m\rangle^2 \, , \quad n = 2, 3 \tag{3.12b}$$

$$D_q \equiv 2\mathcal{J}(q)\langle 1_m|J_z|2_m\rangle\langle 1_m|J_z|3_m\rangle, \tag{3.12c}$$

so that

$$\mathcal{H}_{zz} = \sum_q [A_{2q} a_{q2}^\dagger a_{q2} - B_{2q}(a_{q2}a_{-q2} + a_{q2}^\dagger a_{-q2}^\dagger)$$

$$+ A_{3q} a_{q3}^\dagger a_{q3} - B_{3q}(a_{q3}a_{-q3} + a_{q3}^\dagger a_{-q3}^\dagger)$$

$$- D_q(a_{q2}^\dagger a_{q3} + a_{q2}a_{q3}^\dagger + a_{q2}a_{-q3} + a_{q2}^\dagger a_{-q3}^\dagger)] \, . \tag{3.13}$$

If one did not have the final term coupling the modes from $|2_m\rangle$ and $|3_m\rangle$, the mode energies would be

$$E_{nq} = (A_{nq}^2 - 4B_{nq}^2)^{1/2} = \{\epsilon_n[\epsilon_n - 4\mathcal{J}(q)\langle 1_m|J_z|n_m\rangle^2]\}^{1/2}, \quad n = 2, 3 \tag{3.14}$$

and the generating operators for these modes would be

$$\alpha_{qn}^\dagger = w_{nq} a_{qn}^\dagger + c_{nq} a_{-qn} \, , \quad n = 2, 3 \tag{3.15}$$

with

$$w_{nq} = 2B_{nq}[4B_{nq}^2 - (A_{nq} - E_{nq})^2]^{-1/2}, \quad n = 2, 3 \tag{3.16a}$$

$$c_{nq} = [(A_{nq} - E_{nq})/2B_{nq}]\, w_{nq} \, . \tag{3.16b}$$

We can express $\mathcal{H}_{zz}$ as

$$\mathcal{H}_{zz} = \sum_q [E_{2q}\alpha_{q2}^\dagger \alpha_{q2} + E_{3q}\alpha_{q3}^\dagger \alpha_{q3}$$

$$+ P_q(\alpha_{q2}^\dagger \alpha_{q3} + \alpha_{q2}\alpha_{q3}^\dagger + \alpha_2 \alpha_{-q3} + \alpha_{q2}^\dagger \alpha_{-q3}^\dagger)] \, , \tag{3.17}$$

with

$$P_q \equiv -D_q(w_{2q} - c_{2q})(w_{3q} - c_{3q}) \, . \tag{3.18}$$

Upon considering the commutation relationships for $(\alpha_{q2}^\dagger \pm \alpha_{-q2})$ and $(\alpha_{q3}^\dagger \pm \alpha_{-q3})$ with $\mathcal{H}_{zz}$,

$$[\mathcal{H}_{zz}, \ \alpha_{qn}^\dagger + \alpha_{-qn}] = E_{nq}(\alpha_{qn}^\dagger - \alpha_{-qn}), \quad n = 2, 3 \tag{3.19a}$$

$$[\mathcal{H}_{zz}, \ \alpha_{qn}^\dagger - \alpha_{-qn}] = E_{nq}(\alpha_{qn}^\dagger + \alpha_{-qn})$$

$$+ 2P_q \sum_{m=2,3} (1 - \delta_{mn})(\alpha_{qm}^\dagger + \alpha_{-qm}) \, , \tag{3.19b}$$

one recognizes that the generating operators for the eigenmodes of $\mathcal{H}_{zz}$ are linear combinations of these four operators. The resulting 4×4 secular determinant has the solution

$$E_q^2 = \tfrac{1}{2}(E_{2q}^2 + E_{3q}^2) \pm \tfrac{1}{2}[(E_{2q}^2 - E_{3q}^2)^2 + 16E_{2q}E_{3q}P_q^2]^{1/2} \, . \tag{3.20}$$

Now for the case at hand the Γ_3 states lie well above the Γ_4 states. Since $\langle 1_m|J_z|3_m\rangle$ is nonzero only because $|1_m\rangle$ and $|3_m\rangle$ contain an admixture of $|\Gamma_{4b}\rangle$ [as seen from the molecular-field wave functions of (2.14)], the substantial separation in energy between Γ_3 and Γ_4 means that the admixture is sufficiently small so that $\langle 1_m|J_z|3_m\rangle \ll \langle 1_m|J_z|2_m\rangle$. Thus, the presence of state $|3_m\rangle$ has little effect on the energy values given by the negative sign in front of the square root in (3.20), and these mode energies are very close to those given by E_{2q} of (3.14). [Including $|3_m\rangle$ in the calculation so that the energy is determined by (3.20) (with the minus sign in front of the square root) for numbers corresponding to the states in (2.14) and $\mathcal{J}(0)$ given by (2.13b) gives an E for $q = 0$ about 3 to 4% lower than that given by E_{2q} of (3.14).] Also, in this weak-interaction case, $\langle 1_m|J_z|3_m\rangle$ is sufficiently small so that

$$\mathcal{J}(0)\langle 1_m|J_z|2_m\rangle\langle 1_m|J_z|3_m\rangle \quad ,$$

as well as $\mathcal{J}(0)\langle 1_m|J_z|3_m\rangle^2$, is negligible compared

to ϵ_3. Thus, the roots given by the plus sign in front of the radical in (3.22) have very little dispersion and are almost exactly equal to ϵ_3. (The difference typically is less than 0.1%.) Since there is very little magnetic dipole coupling of state $|3_m\rangle$ to state $|1_m\rangle$, these modes are expected to be weakly excited in comparison to those given by E_{2q} and quite likely are unobservable. In Sec. III C, we shall make use of these observations in comparing the theoretically predicted behavior to the experimental results.

The Bogoliubov-type treatment is expected to be quite good at $T=0$. As something of a check on this, we calculated the mode energies *using the same adjustable parameters as the experimental input in the real cases of interest, i.e., the magnetization at $T=0$ and the crystal-field splitting,* for the Bogoliubov-type calculation and for the pseudospin treatment[9] in the RPA. This was done for the singlet-singlet problem. For a $T=0$ magnetization $\langle J\rangle/\alpha = 0.148$, this gave the $q=0$ mode energy at $T=0$ for the Bogoliubov-type treatment as $E_0/\Delta = 0.150$; while the pseudospin RPA treatment gave $E_0/\Delta = 0.155$. (Here the notation is that of Wang and Cooper.[9] α is the matrix element of J_z between the two crystal-field singlets, and Δ is their splitting.) Thus the difference is indeed quite small.

B. Transverse Excitons

By a treatment analogous to that leading to (3.10) for the longitudinal excitons, we find that the boson Hamiltonian determining the transverse excitation energies is

$$\mathcal{H}_{+-} = \epsilon_4 \sum_i a_{i4}^\dagger a_{i4} + \epsilon_6 \sum_i a_{i6}^\dagger a_{i6} + \epsilon_5 \sum_i a_{i5}^\dagger a_{i5} + \epsilon_7 \sum_i a_{i7}^\dagger a_{i7}$$
$$- \sum_{i\neq j} \mathcal{J}_{ij} [\langle 1_m|J_+|4_m\rangle a_{i4} + \langle 1_m|J_+|5_m\rangle a_{i5} + \langle 6_m|J_+|1_m\rangle a_{i6}^\dagger + \langle 7_m|J_+|1_m\rangle a_{i7}^\dagger]$$
$$\times [\langle 4_m|J_-|1_m\rangle a_{j4}^\dagger + \langle 5_m|J_-|1_m\rangle a_{j5}^\dagger + \langle 1_m|J_-|6_m\rangle a_{j6} + \langle 1_m|J_-|7_m\rangle a_{j7}] \quad . \tag{3.21}$$

For the values of x near the point-charge value of $x=-0.877$, the Γ_5 state lies well above the Γ_4 state. The same type of reasons that we gave in Sec. III A to show that the strongly magnetic-dipole-excited longitudinal excitons with appreciable dispersion involved essentially only the interaction between the molecular-field ground state $|1_m\rangle$ and the lowest-lying molecular-field state (the parentage of which is predominantly Γ_4) applies here. The strongly magnetic-dipole-excited transverse excitons involve states $|4_m\rangle$ and $|6_m\rangle$, the parentage of which is predominantly Γ_4 [see (2.14)], while states $|5_m\rangle$ and $|7_m\rangle$ give rise to sharp but weakly excited levels very close to the molecular field energies ϵ_5 and ϵ_7

Keeping only the terms in (3.21) involving states $|4_m\rangle$ and $|6_m\rangle$, on Fourier transforming with a modest amount of algebra one obtains the mode energies,

$$E_q = \pm\tfrac{1}{2}[\epsilon_4 - \epsilon_6 - (\langle 1_m|J_+|4_m\rangle^2 - \langle 6_m|J_-|1_m\rangle^2)\mathcal{J}(q)]$$
$$+\tfrac{1}{2}\{[\epsilon_4 - \epsilon_6 - (\langle 1_m|J_+|4_m\rangle^2 - \langle 6_m|J_+|1_m\rangle^2)\mathcal{J}(q)]^2$$
$$+ 4\epsilon_4\epsilon_6 - 4\langle 1_m|J_+|4_m\rangle^2\epsilon_6\mathcal{J}(q) - 4\langle 6_m|J_+|1_m\rangle^2\epsilon_4\mathcal{J}(q)\}^{1/2} \quad . \tag{3.22}$$

Note that as $H_{ex}\to 0$ the transverse mode energies of (3.22) approach the longitudinal mode energies of (3.14).

It is important to emphasize that in contrast to the behavior in the singlet-triplet model,[8] there is a finite energy gap at $q=0$. This occurs because the molecular-field states $|1_m\rangle$, $|4_m\rangle$, and $|6_m\rangle$ contain a small admixture of the higher-lying crystal-field states $|\Gamma_{3a}\rangle$, $|\Gamma_{5a}\rangle$, and $|\Gamma_{5c}\rangle$ [see Eq. (2.14)].

C. Model Used for $\mathcal{J}(\vec{q})$ and Comparison of Theoretical Low-Temperature Exciton Dispersion Relationship with Experiment

We have evaluated $\mathcal{J}(0)$ as given in (2.13b) by using molecular-field theory to match the experimental ordered moment per Pr^{3+} in the limit $T=0$, given the experimental crystal-field splitting. To find the theoretical exciton dispersion curves for all $\vec{q}$ we have to either engage in a fairly elaborate fitting of the experimental dispersion curve allow-

ing for exchange constants to as many neighbors as are necessary to fit the data within some experimentally significant accuracy, or we can adopt some simple model for $\mathcal{J}(\vec{q})$, and see how well that fits the data. The fact that the experimental data are on a powder sample, thereby giving a dispersion relationship averaged over direction, provides some motivation to take the latter course, and we have adopted a simple model for $\mathcal{J}(q)$. Indeed, there is a second stronger reason for doing this. This is to emphasize that, without introducing any further adjustable parameters, one was able to anticipate with high accuracy the results of the low-temperature exciton dispersion experiments for Pr_3Tl. With this in mind, we show the results of calculations done prior to the experiments, with $\mathcal{J}(\vec{q})$ given by nearest-neighbor-only exchange for an fcc lattice. We do not, of course, expect such a simple form of the exchange interaction to hold in practice. Indeed, for the metallic systems of interest, the exchange is probably rather long range. However, this simple model for $\mathcal{J}(\vec{q})$ allows us to proceed with no further adjustable parameters. [Actually, for long wavelengths the behavior is not sensitive to the details of the model for $\mathcal{J}(\vec{q})$]. The fact that, as we shall see, calculations done on this basis some months before the experiments were able to predict the experimental results for Pr_3Tl quite accurately tells us two things. First, some features of the low-temperature theoretical dispersion curves are sufficiently sensitive to the details of the mixing of the crystal-field states within the molecular-field states (especially the energy gap as $\vec{q} \to 0$) that we feel we are correctly recognizing the nature of the experimentally observed excitons, and that the present theory describing the behavior of those excitons in the limit of zero temperature works quite well. The second point is that our good understanding of the low-temperature behavior, in effect, emphasizes our puzzlement in not being able to understand the lack of temperature dependence in the experimental dispersion curves.

For nearest-neighbor-only exchange in an fcc lattice $\mathcal{J}(\vec{q})$ is given by:

$$\vec{q} \parallel \langle 111 \rangle, \quad \mathcal{J}(q) = 6\mathcal{J}[\cos(qa/\sqrt{3}) + 1], \quad 0 \le qa \le 3\pi \qquad (3.23a)$$

$$\vec{q} \parallel \langle 110 \rangle, \quad \mathcal{J}(q) = 2\mathcal{J}[\cos(qa/\sqrt{2}) + 1 + 4\cos(qa/2\sqrt{2})], \quad 0 \le qa \le \tfrac{3}{2}\sqrt{2}\pi \qquad (3.23b)$$

$$\vec{q} \parallel \langle 100 \rangle, \quad \mathcal{J}(q) = 4\mathcal{J}[2\cos(\tfrac{1}{2}qa) + 1], \quad 0 \le qa \le 2\pi. \qquad (3.23c)$$

The value of $\mathcal{J}$ is obtained from $\mathcal{J}(0)$ of (2.13b). [In using the $\mathcal{J}(q)$ of (3.23) we do not make a distinction between the fcc lattice and the Cu_3Au lattice, where four of the nearest neighbors to a Pr are Tl. Since we always use the $\mathcal{J}(0)$ necessary to give the experimental magnetization at $T = 0$, this allows us to arrive, in a convenient and physically reasonable way, at a $\mathcal{J}(q)$ that has the over-all cubic symmetry correct for the Cu_3Au lattice, while avoiding the complications associated with the fact that there are three inequivalent types of Pr sites each having locally tetragonal symmetry.]

Using $\mathcal{J}(q)$ given by (3.23) in Eqs. (3.14) and (3.22), with the various matrix elements of J_z, J_+, and J_- determined using the molecular-field states of (2.14), gives the longitudinal and transverse exciton curves shown in Fig. 4. For the longitudinal modes one also predicts a weak, but sharp, spectrum coming from state $|3_m\rangle$ for $E \approx 127\,^\circ$K; and for the transverse modes, weak but sharp states corresponding to $|5_m\rangle$ and $|7_m\rangle$ at $E \approx 158$ and $182\,^\circ$K.

To check the sensitivity of the results to use of a different value for the $T = 0$ magnetization M_0, we have also repeated the calculations for $M_0 = 0.87\mu_B$ (i.e., a 16% increase in M_0). This leads to an increase in the $q = 0$ gap for the longitudinal modes from 12.2 to 14.4 °K and for the transverse modes from 17.8 to 20.8 °K, while the energies at the maximum q are almost unchanged. Also we varied x slightly from the point-charge value to see how the excitation energy changed. Keeping the other parameters fixed, for $x = -1$ the lowest-lying excitation energy increased by about 3% over the value at $x = -0.877$.

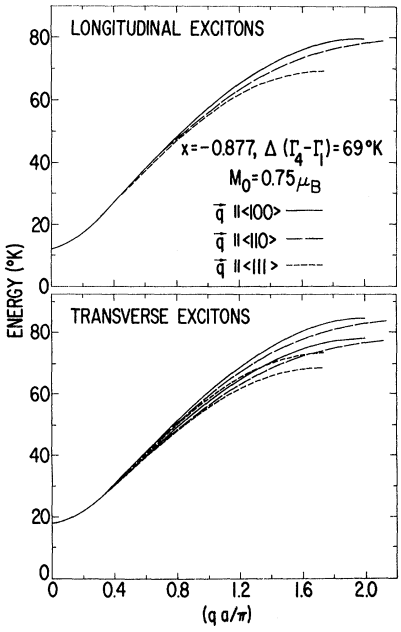

FIG. 4. Theoretical dispersion curves for magnetic excitons at $T = 0$ in Pr_3Tl and fcc Pr with $x = -0.877$, $\Delta(\Gamma_4 - \Gamma_1) = 69\,^\circ$K, and $M_0 = 0.75\mu_B$.

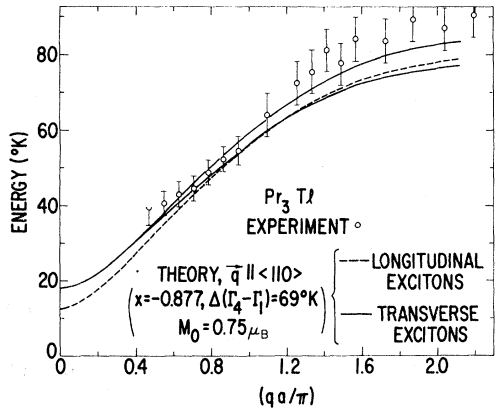

FIG. 5. Comparison of theory and experiment for magnetic-exciton dispersion in Pr_3Tl. Data are those of Ref. 14.

Again, we emphasize the importance of the admixture of the $|\Gamma_5\rangle$ and $|\Gamma_3\rangle$ states into the molecular-field states of predominantly $|\Gamma_1\rangle$ and $|\Gamma_4\rangle$ parentage to obtain the results of Fig. 4. If there was no $|\Gamma_5\rangle$ admixture, the energy gap for transverse excitons would disappear. If the $|\Gamma_3\rangle$ admixture was neglected in finding the longitudinal mode energies, the energy gap at $q=0$ would increase by about 75%.

In Fig. 5 we compare the theoretical prediction [where the only adjustable parameters are $x=-0.877$ (point-charge value), M_0 (moment per Pr at $T=0$) $=0.75\mu_B$, and Δ (Γ_4-Γ_1 crystal-field splitting) $=69\,^\circ$K] to the experimental results of Birgeneau *et al.*[14] for powder samples of Pr_3Tl. (In the plot vs qa, the lattice constant value used for Pr_3Tl is[15] 4.926 Å.) The experimental dispersion curve is essentially unchanged from 4.2 up to 60 °K above which temperature the excitons are no longer observable. [The maximum value of $|q|$ found in the experiments is $|q|=1.4$ Å^{-1}. This is in good agreement with the longest dimension of the first Brillouin for the fcc lattice, from Γ to W, equal to 1.43 Å^{-1} using the lattice constant[15] (4.926 Å) of Pr_3Tl.] In Fig. 5 for visual clarity we show only the theoretical curves for $\vec{q}\parallel\langle 110\rangle$. The average dispersion curve for a powder sample is probably rather close to the average of the three $\langle 110\rangle$ curves shown. The agreement between theory and experiment is strikingly good. Using a Δ somewhat higher than 69 °K would make the agreement even somewhat better. (The experimental[14] dispersion curve for fcc Pr is considerably flatter than that for Pr_3Tl. Since, as already stated, there are peculiarities in the magnetic ordering of fcc Pr, we do not attempt to explain this.) Not surprisingly, there is no experimental indication of the sharp weak modes corresponding to states $|3_m\rangle$, $|5_m\rangle$, and $|7_m\rangle$.

IV. EXCITATION SPECTRUM FOR x NEAR Γ_4-Γ_5 CROSSING

As shown in Fig. 1, the Γ_4 and Γ_5 crystal-field levels cross at $x=-0.375$. We investigated the exciton behavior near this crossing to see how much different this would be from the behavior near the point-charge model value for x. This was done with the thought that having the Γ_5 level near the Γ_4 level might be involved somehow in the puzzling temperature dependence (i.e., lack thereof) of the dispersion behavior. The dispersion behavior expected near the Γ_4-Γ_5 crossing is indeed quite different; however, this does not appear to be of help in understanding the anomalous behavior. Nevertheless, to complete our discussion we briefly present these results. The neutron observations[30] seem to eliminate the possibility of the Γ_5 level falling below the Γ_4 level, so we considered $x=-0.425$, where Γ_5 is slightly above Γ_4. The Γ_4-Γ_1 splitting has been kept at the value of 69 °K used in the $x=-0.877$ calculations.

As already pointed out, so long as the Γ_4-Γ_1 splitting is kept constant, the longitudinal mode behavior is unchanged. On the other hand, in this x regime where strong Γ_4-Γ_5 mixing is expected, the full Hamiltonian of (3.21) must be used in finding the transverse mode behavior.

To find the modes of $\mathcal{H}_{+-}$ given by (3.21) we first find the Hamiltonian in terms of Fourier-transformed boson operators, i.e., as given by (3.11). Next we separately diagonalize the parts of the Hamiltonian involving only $|4m\rangle$ and $|6m\rangle$ and only $|5m\rangle$ and $|7m\rangle$. For the $|4m\rangle$, $|6m\rangle$ terms this means diagonalizing

$$\mathcal{H}_{46}=\sum_q\{[\epsilon_4-\eta_4^2\mathcal{J}(q)]a_{4q}^\dagger a_{4q}+[\epsilon_6-\eta_6^2\mathcal{J}(q)] \times a_{6q}^\dagger a_{6q}-\eta_4\eta_6\mathcal{J}(q)(a_{4q}^\dagger a_{6-q}^\dagger+a_{4q}a_{6-q})\}, \quad (4.1)$$

where for convenience we define

$$\eta_4\equiv\langle 1_m|J_+|4_m\rangle=\langle 4_m|J_-|1_m\rangle, \quad (4.2a)$$

$$\eta_6\equiv\langle 6_m|J_+|1_m\rangle=\langle 1_m|J_-|6_m\rangle, \quad (4.2b)$$

$$\eta_5\equiv\langle 1_m|J_+|5_m\rangle=\langle 5_m|J_-|1_m\rangle, \quad (4.2c)$$

$$\eta_7\equiv\langle 7_m|J_+|1_m\rangle=\langle 1_m|J_-|7_m\rangle; \quad (4.2d)$$

while for $|5_m\rangle$ and $|7_m\rangle$ one makes the replacement $4\rightarrow 5$ and $6\rightarrow 7$ to define $\mathcal{H}_{57}$.

The generating operators diagonalizing $\mathcal{H}_{46}$ are

$$\alpha_{q1,2}^\dagger=w_{q1,2}a_{4q}^\dagger+c_{q1,2}a_{6-q}^\dagger, \quad (4.3)$$

where

$$w_{q1,2}=B_{46q}/[B_{46q}^2-(A_{4q}-E_{46q1,2})^2]^{1/2}, \quad (4.4a)$$

$$c_{q1,2}=[(A_{4q}-E_{46q1,2})/B_{46q}]\,w_{q1,2}, \quad (4.4b)$$

with

$$A_{4q}\equiv\epsilon_4-\eta_4^2\mathcal{J}(q), \quad (4.5a)$$

$$B_{46q} = -\eta_4\eta_6 \mathcal{J}(q), \tag{4.5b}$$

and the energy eigenvalues of $\mathcal{H}_{46}$ are

$$E_{46q1,2} = -\tfrac{1}{2}(A_{6q} - A_{4q}) \pm [(A_{6q} + A_{4q})^2 - B_{46q}^2]^{1/2}, \tag{4.6}$$

where

$$A_{6q} = \epsilon_6 - \eta_6^2 \mathcal{J}(q). \tag{4.7}$$

[If E_{46q} in (4.4) is negative, the absolute value should be taken of the quantity within the brackets in the denominator.] The replacement $4 \to 5$, $6 \to 7$ serves to define the generating operators

$$\beta_{q1,2}^\dagger = t_{q1,2} a_{5q}^\dagger + s_{q1,2} a_{7-q}^\dagger \tag{4.8}$$

and eigenvalues E_{57q} diagonalizing $\mathcal{H}_{57}$.

Then $\mathcal{H}_{+-}$ can be written in terms of the $\alpha_{q1,2}$ and $\beta_{q1,2}$,

$$\mathcal{H}_{+-} = \sum_q [E_{46q1}\alpha_{q1}^\dagger\alpha_{q1} + E_{46q2}\alpha_{q2}^\dagger\alpha_{q2} + E_{57q1}\beta_{q1}^\dagger\beta_{q1} + E_{57q2}\beta_{q2}^\dagger\beta_{q2}$$
$$+ D_{q1}(\alpha_{q1}\beta_{q1}^\dagger + \alpha_{q1}^\dagger\beta_{q1}) + D_{q2}(\alpha_{q1}\beta_{q2}^\dagger + \alpha_{q1}^\dagger\beta_{q2}) + D_{q3}(\alpha_{q2}\beta_{q1}^\dagger + \alpha_{q2}^\dagger\beta_{q1}) + D_{q4}(\alpha_{q2}\beta_{q2}^\dagger + \alpha_{q2}^\dagger\beta_{q2})], \tag{4.9}$$

with

$$D_{q1} = -K(q)(-\eta_4\eta_7 c_{q2}t_{q2} + \eta_4\eta_5 c_{q2}s_{q2} - \eta_5\eta_6 w_{q2}s_{q2} + \eta_6\eta_7 w_{q2}t_{q2}), \tag{4.10a}$$

$$D_{q2} = -K(q)(\eta_4\eta_7 c_{q2}t_{q1} - \eta_4\eta_5 c_{q2}s_{q1} + \eta_5\eta_6 w_{q2}s_{q1} - \eta_6\eta_7 w_{q2}t_{q1}), \tag{4.10b}$$

$$D_{q3} = -K(q)(\eta_4\eta_7 c_{q1}t_{q2} - \eta_4\eta_5 c_{q1}s_{q2} + \eta_5\eta_6 w_{q1}s_{q2} - \eta_6\eta_7 w_{q1}t_{q2}), \tag{4.10c}$$

$$D_{q4} = -K(q)(-\eta_4\eta_7 c_{q1}t_{q1} + \eta_4\eta_5 c_{q1}s_{q1} - \eta_5\eta_6 w_{q1}s_{q1} + \eta_6\eta_7 w_{q1}t_{q1}), \tag{4.10d}$$

where

$$K(q) \equiv \mathcal{J}(q)/(w_{q1}c_{q2} - w_{q2}c_{q1})(t_{q1}s_{q2} - t_{q2}s_{q1}). \tag{4.11}$$

For each q, the four eigenvalues of $\mathcal{H}_{+-}$ are the roots of the 4×4 secular determinant,

$$0 = \begin{vmatrix} (E_{46q1}-E) & 0 & D_{q1} & D_{q2} \\ 0 & (E_{46q2}-E) & D_{q3} & D_{q4} \\ D_{q1} & D_{q3} & (E_{57q1}-E) & 0 \\ D_{q2} & D_{q4} & 0 & (E_{57q2}-E) \end{vmatrix}. \tag{4.12}$$

Figure 6 shows the dispersion curves for $x = -0.425$, $\Delta = 69\,^\circ\mathrm{K}$, $M_0 = 0.76\mu_B$, with $\vec{q}$ along a $\langle 110\rangle$ direction. There is sufficient mixing of the third branch (i.e., ordering the branches with increasing energy) with the lower two branches for us to expect that branch to be excited with significant intensity in magnetic-dipole transitions. This appears to be incompatible with the observed excitation spectrum.[30] This, coupled with the good agreement shown in Fig. 5 between the experimental spectrum and the theoretical prediction for $x = -0.877$, indicates that the value of x for Pr_3Tl, and also probably for fcc Pr, is in the neighborhood of the point-charge value, i.e., where fourth-order anisotropy is predominant.

V. TEMPERATURE DEPENDENCE OF EXCITATION SPECTRA

The effective boson (i.e., Bogoliubov-type) theory used in Secs. III and IV to calculate the excitation spectra shown in Figs. 4–6 is valid only in the limit of zero temperature. However, we can use the results found by Wang and Cooper[9] for the singlet-singlet problem using the pseudospin treatment in the RPA as a guide to discuss the expected temperature dependence. On this basis we now discuss the expected temperature dependence for the excitation spectra with $x = -0.877$ as shown in the limit $T = 0$ in Fig. 4 and compared to experiment in Fig. 5.

From the RPA pseudospin singlet-singlet results we expect that as T approaches T_C, the $q = 0$ longitudinal and transverse mode energies drop and approach each other as they go to zero at T_C. Above T_C, the behavior eventually becomes that for the allowed crystal-field transitions with intensities determined by the thermal population. The weak sharp modes expected at ϵ_3, ϵ_5, and ϵ_7 are expected to become weaker and sharper, disappearing at T_C.

The experimental behavior[14] shows no evidence of soft-mode behavior on approaching T_C. Indeed, there is essentially no temperature variation of the observed dispersion behavior up to $\sim 60\,^\circ\mathrm{K}$, above which temperature the excitons are no longer observable.

As a guide[29] to the fraction of the Brillouin zone over which mode softening might be observable, we calculated the change in the Bogoliubov-type boson spectrum at $T = 0$ as the exchange, and hence the ordered moment decreased. This is shown in Fig. 7 for the longitudinal excitons for $x = -0.877$, $\Delta = 69\,^\circ\mathrm{K}$, but decreasing H_{ex} and $\mathcal{J}(0)$ so that M_0 decreases to values equal to about $\frac{1}{2}$ and $\frac{1}{3}$ of the value $(0.75\,\mu_B)$ pertinent to Figs. 4 and 5. We realize, of course, that this does not give us the change

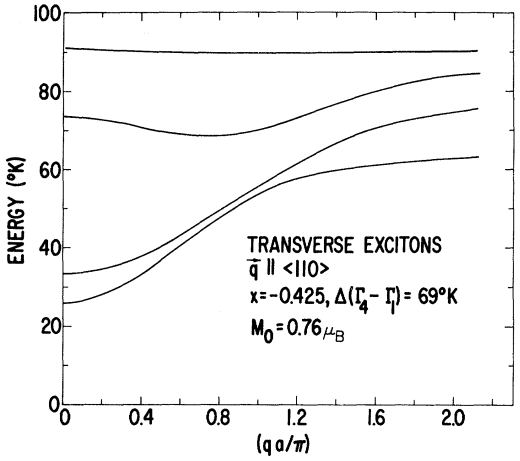

FIG. 6. Theoretical dispersion curves for transverse magnetic excitons at $T=0$ in Pr_3Tl and fcc Pr with $x=-0.425$, $\Delta(\Gamma_4-\Gamma_1)=69\,^{\circ}\mathrm{K}$, and $M_0=0.76\mu_B$.

with temperature for fixed $\mathcal{J}(0)$ on going toward T_C; but it was felt that the results found could serve as a gauge to see if one might reasonably expect to see effects over enough of the Brillouin zone to be experimentally observable. The only significant change in mode energies as shown in Fig. 7 occurs at quite low q. (For this x value, the softening of the transverse modes for the same change in exchange at $T=0$ is quite comparable.) Nevertheless, had there been effects of this size, and if the mode softening had involved an approach to linear variation of E with q at low q, these effects could have been detected experimentally.[30] Such an approach to linear variation of E with q, associated with mode softening, is found in the RPA treatment[9] of the temperature-dependent behavior for the singlet-singlet model, and is also found in the $T=0$ behavior with decreasing exchange shown in Fig. 7.

In Fig. 8, we show the results of the same sort of decrease in M_0 at $x=-0.425$. Note, however, that one has to decrease M_0 to much smaller values than at $x=-0.877$ in order to get strong softening of the small q modes. This comes about because of a combination of two effects. First is the important point that according to present theories it is the softening of the longitudinal modes that drives the transition to magnetic disordering. The transverse modes are driven soft only because the effective molecular field mixing the crystal-field states disappears at the Curie temperature. Second, at $x=-0.425$ these transverse modes involve a much larger admixture of Γ_5 states into the Γ_4 states than at $x=-0.877$. It is only when this admixture becomes very small that appreciable mode softening for small q finally occurs. Actually, the Γ_4-Γ_5 mixing effects are so strong for M_0, as small as $0.21\mu_B$ (corresponding to $H_{ex}=2.54\times10^4$ Oe), that the $q=0$ energy gap is almost constant between $M_0=0.76\mu_B$ and $M_0=0.21\mu_B$, and actually is slightly larger at $M_0=0.21$ than at $M_0=0.76\mu_B$ before starting to decrease for smaller M_0. *These strong mixing effects for small exchange fields suggest that it may be interesting to see the applied magnetic-field effects on the excitation spectrum. Observation of such effects, or the lack thereof, could further confirm our identification of the x value as corresponding to predominantly fourth-order anisotropy.*

It is tempting to raise the possibility that the ef-

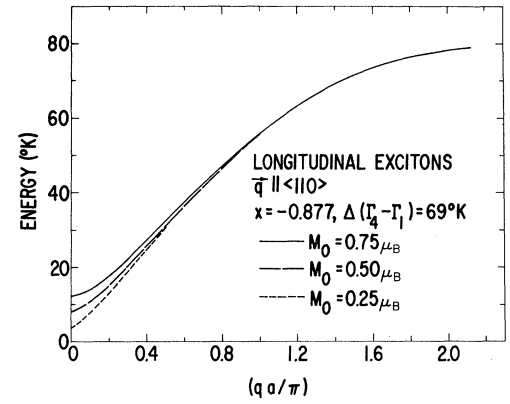

FIG. 7. Theoretical dispersion curves for longitudinal magnetic excitons at $T=0$ in Pr_3Tl and fcc Pr for $M_0=0.75\mu_B$, $0.50\mu_B$, and $0.25\mu_B$ with $x=-0.877$ and $\Delta(\Gamma_4-\Gamma_1)=69\,^{\circ}\mathrm{K}$.

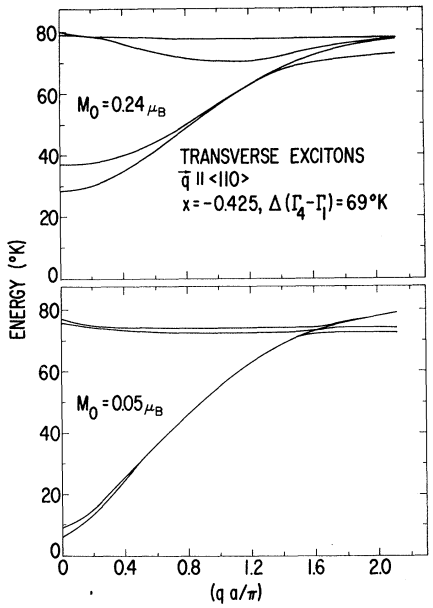

FIG. 8. Theoretical dispersion curves for transverse magnetic excitons at $T=0$ in Pr_3Tl and fcc Pr for $M_0=0.24\mu_B$ and $0.05\mu_B$ with $x=-0.425$ and $\Delta(\Gamma_4-\Gamma_1)=69\,^{\circ}\mathrm{K}$.

fective field mixing the crystal-field states, and thereby leading to an energy gap at $q = 0$ for the transverse modes, is not identical with a molecular field that disappears when magnetic ordering disappears (i.e., some sort of effective mixing field associated with short-range order). Thus, one might rationalize the absence of significant softening of the transverse modes at T_C. However, this does not seem tenable as an explanation of the experimentally observed behavior, since one would in any case expect to observe the softening of the longitudinal modes. Also, the fact that the experimental dispersion relationship is essentially unchanged at a temperature four times the Curie temperature in Pr_3Tl does not seem amenable to this point of view.

Thus present theory is quantitatively extremely successful in predicting the low-temperature magnetic-exciton behavior in Pr_3Tl, and is quite unsuccessful in predicting the lack of temperature dependence of the exciton dispersion relationships.[31] Finally, we must point out that in neutron-inelastic-scattering experiments on single-crystal dhcp Pr performed by Rainford and Houmann[13] the optic exciton at Γ has an energy that is considerably lower at 4.2 °K than at 18 °K. Since single-crystal dhcp Pr is paramagnetic at all temperatures, Rainford and Houmann point out that this is in at least qualitative agreement with the predictions of Wang and Cooper[9] for mode softening. Measurements at temperatures intermediate to 4.2 and 18 °K are desirable to verify whether indeed one has mode softening in the expected way for dhcp Pr. If one does verify the mode softening, it is very difficult to understand why dhcp Pr on the one hand and Pr_3Tl and fcc Pr on the other should behave qualitatively quite differently with regard to the presence of mode softening. There is certainly no reason in principle why the mode softening in Pr_3Tl on decreasing temperature from 60 °K down to the Curie temperature of 11 °K should behave qualitatively differently than the mode softening in dhcp Pr on going from 18 °K to a very low temperature. Obviously, it is quite desirable to have single crystals of a singlet-ground-state ferromagnet like Pr_3Tl or fcc Pr. Then one could measure the complete exciton dispersion curves, and one could feel complete confidence that the presence or absence of mode softening was experimentally verified.

ACKNOWLEDGMENTS

The author is grateful to Miss E. L. Kreiger for her assistance with the numerical calculations. He has benefited from discussions with several of the authors of the experimental papers on Pr_3Tl and fcc Pr: R. J. Birgeneau, J. Als-Nielsen, K. Andres, and E. Bucher; but he is especially grateful to R. J. Birgeneau for a number of extensive discussions before, during, and after the neutron-scattering experiments, that helped to stimulate the author's interest and helped in formulating the discussion given in the present paper.

[1]For a review of singlet-ground-state magnetism, see, B. R. Cooper and O. Vogt, J. Phys. (Paris) 32, C1-958 (1971); also see B. R. Cooper, CRC Critical Reviews in Solid State Sci. 3, 83 (1972).

[2]G. T. Trammell, J. Appl. Phys. 31, 362S (1960).

[3]G. T. Trammell, Phys. Rev. 131, 932 (1963).

[4]B. Bleaney, Proc. Roy. Soc. (London) 276A, 19 (1963).

[5]B. R. Cooper, Phys. Rev. 163, 444 (1963).

[6]R. M. Bozorth and J. H. Van Vleck, Phys. Rev. 118, 1493 (1960).

[7]Y. Kitano, F. Specht, and G. T. Trammell, in *Proceedings of the International Conference on Magnetism, Nottingham*, 1964 (Institute of Physics and the Physical Society, London, 1965), p. 480.

[8]B. Grover, Phys. Rev. 140, A1944 (1965).

[9]Y.-L. Wang and B. R. Cooper, Phys. Rev. 172, 539 (1968); 185, 696 (1969).

[10]D. Pink, J. Phys. C 1, 1246 (1968).

[11]B. R. Cooper and O. Vogt, Phys. Rev. B 1, 1218 (1970).

[12]T. M. Holden, W. J. L. Buyers, E. C. Svensson, and O. Vogt, Bull. Am. Phys. Soc. 16, 325 (1971).

[13]B. R. Rainford and J. Gylden Houmann, Phys. Rev. Letters 26, 1254 (1971).

[14]R. J. Birgeneau, J. Als-Nielsen, and E. Bucher, Phys. Rev. Letters 27, 1530 (1971).

[15]R. J. Birgeneau, J. Als-Nielsen, and E. Bucher, preceding paper, Phys. Rev. B 6, 2724 (1972).

[16]O. Vogt and B. R. Cooper, J. Appl. Phys. 39, 1202 (1968).

[17]B. R. Cooper and O. Vogt, Phys. Rev. B 1, 1211 (1970).

[18]R. J. Birgeneau, E. Bucher, L. Passell, and K. C. Turberfield, Phys. Rev. B 4, 718 (1971).

[19]S. Foner, B. R. Cooper, and O. Vogt, Phys. Rev. B 6, 2040 (1972).

[20]R. J. Birgeneau, E. Bucher, L. Passell, D. L. Price, and K. C. Turberfield, J. Appl. Phys. 41, 900 (1970).

[21]K. C. Turberfield, L. Passell, R. J. Birgeneau, and E. Bucher, J. Appl. Phys. 42, 1746 (1971).

[22]K. Andres, E. Bucher, S. Darack, and J. P. Maita, second preceding paper, Phys. Rev. B 6, 2716 (1972).

[23]E. Bucher, J. P. Maita, and A. S. Cooper, third preceding paper, Phys. Rev. B 6, 2709 (1972).

[24]E. Bucher, C. W. Chu, J. P. Maita, K. Andres, A. S. Cooper, E. Buehler, and K. Nassau, Phys. Rev. Letters 22, 1260 (1969).

[25]K. R. Lea, M. J. M. Leask, and W. P. Wolf, J. Phys. Chem. Solids 23, 1381 (1962).

[26]These expressions were originally derived for use in a study of $TmAl_3$: B. R. Cooper, Helv. Phys. Acta 41, 750 (1968); and (unpublished).

[27]A. J. Freeman and R. E. Watson, Phys. Rev. 127, 2058 (1962).

[28]For an excellent review of the various approaches to the crystal-field formalism and the point-charge model see M. T. Hutchings, *Solid State Physics*, edited by F. Seitz and D. Turnbull (Academic, New York, 1964), Vol. 16, p. 227.

[29]R. J. Birgeneau, J. Als-Nielsen, and E. Bucher (private communication).

[30]The discussion of these points, and a number of others in this paper, has benefited from extensive discussions with R. J. Birgeneau before, during, and after the neutron experiments of Refs. 14 and 15.

[31]A letter by S. R. P. Smith (to appear in J. Phys. C.) was received subsequent to submission of the present paper. This letter reports calculations giving a temperature dependence of the mode energies in the singlet-triplet case that is fundamentally different from the behavior for the singlet-singlet case. In particular, there is no soft-mode behavior. It is not obvious that even such singlet-triplet behavior would explain the experimental lack of temperature dependence for the exciton dispersion. Calculations along similar lines by Y. Y. Hsieh [(unpublished), also received subsequent to submission of the present paper] should help in verifying the correctness of Smith's results, and in judging the relevance to the experimental situation.

PHYSICAL REVIEW B VOLUME 6, NUMBER 7 1 OCTOBER 1972

Electronic Interactions in the $4f^6\,5d$ Configuration of Eu^{2+} in Crystals

Herbert A. Weakliem
RCA Laboratories, Princeton, New Jersey 08540
(Received 11 May 1972)

The electronic coupling in the $4f^6\,5d$ configuration of Eu^{2+} in crystals has been studied. The complete f-d Coulomb matrix within $f^6\,(^7F_J)\,^2e_g$ has been obtained and the Hamiltonian diagonalized for various values of the spin-orbit and Coulomb parameters. The magneto-optical spectra in the first band and the g values of the 4130-Å resonance line of $CaF_2:Eu^{2+}$ are quite well explained by using f-d Coulomb interaction about one-half that of the free ion. Even this reduced interaction is by no means negligible and it is shown qualitatively that the same Coulomb f-d parameters are appropriate for EuF_2 as well as $CaF_2:Eu^{2+}$. It is argued that the reduction from the free-ion case is a physically significant result caused by the crystal environment of the ion, and is not merely the result of some neglected configuration interactions.

I. INTRODUCTION

The optical-absorption, emission, and magneto-optical spectra of $CaF_2:Eu^{2+}$ and EuF_2 are rich in detail and have been the subject of numerous studies.[1-8] The absorption spectra contain two bands in the uv, and at low temperatures the lower energy band has considerable structure and strong magneto-optic dichroism.[4-6] The bands are due to allowed electric dipole transitions from the ground state of Eu^{2+}, $4f^7\,(^8S_{7/2})$, to states of the $4f^6\,5d$ configuration. A narrow intense resonance line at 4130 Å is observed in both emission and absorption[1] at 4 °K in $CaF_2:Eu^{2+}$. The excited state of this line is a fourfold degenerate level and is the lowest-energy component state of the $4f^6\,5d$ configuration.[3]

The two bands have been attributed to the cubic crystal field splitting of the $5d$ electron; however, the Coulomb interaction between $5d$ and the $4f^n$ core is not small and this complicates the interpretation of the $4f^n\,5d$ band states. The $4f^n\,5d$ configurations have not been extensively studied, particularly in crystals. Several approximate calculations on $4f^6\,5d$ have been made for Eu^{2+} in order to explain variously the structure in the first band,[8-10] the Faraday effect[4] and magnetic circular dichroism (MCD), and the Zeeman effect of the resonance line.[7] The coupling schemes used have ranged all the way from pure Russell-Saunders zero $5d$ crystal field splitting to strong $5d$ crystal field weak f-d Coulomb interaction. In fact, intermediate coupling is indicated by consideration of various typical energy splittings of the lanthanides: (a) $5d$ crystal fields of 10 000–15 000 cm^{-1}, (b) $4f\,5d$ term splittings of 2000–5000 cm^{-1}, (c) spin-orbit splittings of 2000–5000 cm^{-1}.

We shall show that the spectra and the g values of the excited state of the resonance line are well accounted for by intermediate coupling within $5d$ crystal field configurations. The configurations are formed by coupling the crystal field ^2e_g and $^2t_{2g}$ orbitals of $5d$ to the ^7F ground term of the f^6 core. The full matrix of $f^6\,(^7F_J)\,^2e_g$, including spin-orbit and f-d Coulomb interaction, was diagonalized for various values of the parameters. The effect of configuration interaction with $f^6\,(^7F)^2t_{2g}$ was adequately treated by perturbation theory. We find that the experimental $CaF_2:Eu^{2+}$ data are best explained by using the Coulomb f-d parameters $F_2 = 65$ cm^{-1} and $G_1 = 110$ cm^{-1}, which are approxi-